Environment Impact and Probabilistic Health Risks of PAHs In Dusts Surrounding an Iron and Steel Enterprise

Xiaofeng Wei
Shandong Jianzhu University
Chun Ding
Shandong Jianzhu University
Chunzhu Chen
Shandong Jianzhu University
Li Zhu
Shandong Jianzhu University
Guiqin Zhang
Shandong Jianzhu University
Youmin Sun (ymsun@sdjzu.edu.cn)
Shandong Jianzhu University

Research Article

Keywords: PAHs, environment impact, health risk, dust, iron and steel enterprise

Posted Date: January 11th, 2021

DOI: https://doi.org/10.21203/rs.3.rs-136997/v1

Version of Record: A version of this preprint was published at Scientific Reports on March 24th, 2021. See the published version at https://doi.org/10.1038/s41598-021-85053-4.

Environment impact and probabilistic health risks of PAHs in dusts surrounding an iron and steel enterprise

Xiaofeng Wei · Chun Ding · Chunzhu Chen · Li Zhu ·Guiqin Zhang· Youmin Sun*

School of Municipal and Environmental Engineering, Shandong Jianzhu University, Jinan 250101, Shandong, China

*Corresponding author. Tel.: 13001727629

Email: ymsun@sdjzu.edu.cn

Abstract: Dust can be regarded as environmental medium that indicates the level and spatial distribution of polycyclic aromatic hydrocarbons (PAHs) coming from different pollution sources. In this study, samples including road dust, roof dust, and bare soil near an iron and steel enterprise (ISE) in Laiwu city of North China were collected. To assess the environment impact, atmosphere particulates and one flue dust from a coking plant were simultaneously sampled. Sixteen USEPA PAHs were detected quantitatively by Gas Chromatography Mass Spectrometry(GC-MS). A laser particle size analyzer was used to obtain the grain size of the dust particle samples. The results showed that PAH concentrations displayed great variability in the dust samples. The $\sum_{16}$ PAHs concentration was found to be between 0.460 and 46.970 μg/g (avg ± sd: 10.892 ± 1.185 μg/g) in road dust, between 0.670 and 17.140 μg/g (avg ± sd: 6.751 ± 0.692 μg/g) in roof dust, and 13.990 ± 1.203 μg/g in bare soil. In the environment atmosphere sites, the $\sum_{16}$ PAHs value in $PM_{2.5}$ constituted a very large proportion of PM_{10}, indicating that PAHs in finer particle sizes should be given greater emphasis. The $\sum_{16}$PAHs concentration was relatively high in the area close to the ISE because of the great impact of the ISE industrial activities. PAH concentration curves were similar, and the most abundant individual PAHs in the atmosphere sites were BbF, BkF, and Flu, and BbF, BkF, and Chry in dusts. Toxicity analysis revealed that PAHs with four rings, including carcinogenic PAHs, were the dominant pollutants in the studied area. The toxic equivalency value (TEQ_{BaP}), the carcinogenic health risk assessment value recommended by the US EPA, was calculated for seven carcinogenic PAHs, revealing that they account for more than 93.0% of the total TEQ_{Bap} of the 16 PAHs and indicating the major toxic equivalent concentration contributor. Incremental lifetime cancer risk (ILCR) estimation results showed that PAHs tended to bring about great health risks through skin contact, followed by ingestion and inhalation. By comparison, road dust exhibited greater carcinogenic risks than roof dust, and bare soil may undergo heavier pollution. Therefore, the results of this study would be helpful in the effort to understand the PAHs pollution from the steel industry, which will provide some guidance for the probabilistic assessment of local health risks.

Keywords: PAHs, environment impact, health risk, dust, iron and steel enterprise

Polycyclic aromatic hydrocarbons (PAHs), a class of persistent semi-volatile organic pollutants with characteristics of high toxicity and strong metamorphism, are one of the first discovered environmental carcinogens (Chen et al. 2017; Tsapakis et al. 2005; Sun et al. 2019; Filho et al 2020). PAHs consist of over 200 organic compounds, of which 16 are included in the list of priority controlled pollutants by the United States Environmental Protection Agency (US EPA) in 1976 (Christophe et al. 2006). Numerous studies have revealed the main sources of PAHs to be residential coal burning, garbage incineration, activation of internal combustion engines, and various industrial activities such as coke production, oil refining, aluminum production, and smelting of non-ferrous metals (Cheng et al. 2005). It is reported that PAH pollution in industrial areas is more serious than that in residential areas (Shi et al. 2014); thus, many studies have reported PAH concentrations in the areas surrounding coal storage, coking and power plants, and iron and steel enterprises (ISEs). (Gilio et al. 2017; He et al. 2009). Notably, the ISE performs multiple production steps and long-milling techniques, such as sintering, coking, iron smelting, and steelmaking, and each step

contains several combined processes that lead to PAH pollution (Wang et al. 2014). In China, PAH levels have clear temporal and spatial distribution characteristics. PAH concentrations in winter are significantly higher than in other seasons (Chang et al. 2006; Huang et al. 2006), and in northern cities, they are higher than in southern cities (Lan et al. 2015). Therefore, the PAH level at the ISE of a city in northern China during the winter was chosen for examination.

With improvements in technology, particles and PAHs from tail pipe emissions have been significantly reduced. However, atmospheric PAHs, which escape photo-degradation in the air and treatment from the tail gas equipment can accumulate in environmental media through dry and wet deposition (Takeshi et al. 2018). Moreover, with the expansion of industrialization and urbanization in China, PAH emissions have maintained an increasing trend, which means that the impact of PAHs on society has gradually increased (Sun et al. 2006). Researchers have given attention to the characteristics, concentrations, and sources of PAHs in different environmental media (Cetin et al. 2007; Odabasi et al. 2009). In most of these studies, the status of PAH pollution has been evaluated in the surrounding soil, street dust, water, atmosphere, and other environmental media or biological systems (Kwon et al. 2014; Yang et al. 2002; Tsai et al. 2007, Li et al. 2017), whereas research on PAHs in different types of dust is quite limited. In addition, it is very important to study the influence of PAHs on the surrounding environment in air-dust media.

Shandong Province, as the third largest economic province in China, hosts iron and steel production plants in Laiwu. In the present study, road dust, roof dust, bare soil, and atmosphere particles were collected from the ISE in this city that had an annual production capacity of 3 million tons of fine metal plates, sheets, and strips and 600,000 tons of stainless steel. The concentration level and environmental impact of 16 PAHs in dusts surrounding the ISE were assessed. Furthermore, incremental lifetime carcinogenic risks due to exposure to PAHs in dust were evaluated. These findings can serve as a scientific basis for the control of PAH pollution in the areas surrounding the ISE.

1 Materials and Methods

1.1 Sample sites and collection

Five sample sites surrounding an ISE were selected based on their representativeness of the area in Laiwu City. The detailed information for the sampling sites are as follows: site 1 (S1): coking plant, site 2 (S2): iron smelting plant (including sintering), site 3 (S3): steelmaking plant: site 4 (S4): Daqin Village (located 3.6 km northeast of the nearest ISE boundary), site 5 (S5): Mengjiazhuang (located 2.2 km southwest of the nearest ISE boundary). The dominant wind direction surrounding the ISE is greatly controlled by the northeast and southeast wind in winter (our sampling period).

The spatial distribution of the sampling sites is shown in Fig. 1. Road dust samples were collected at five sites (S1-S5). Roof dust samples were collected at S1, S2, S3, and S5, at height of approximately 10 m, 10 m, 10 m, and 15 m above the ground, respectively. The atmospheric particulate matter (PM) samples (A2, A4, A5) were collected at S2, S4, and S5, at heights of approximately 10 m, 13 m, and 15 m above the ground, respectively. Moreover, bare soils were collected at S3. For each type of sample, at least three samples were collected at the same site. Dust particle samples (A1) emitted from the the ISE coking plant were collected at S1.

Road and roof dust samples were collected using vacuum cleaners (Samsung, SC88P0). Bare soils were collected up to a depth of 20 cm at S3 by shovel. The collected road, roof dust, and bare soil samples were air-dried indoors, sieved through a 150-mesh sieve, and kept for further PAH analysis. Atmospheric PM filter samples ($PM_{2.5}$ and PM_{10}) were collected at A2, A4, and A5 in winter (December 25–30, 2016). Each quartz filter sample (φ90 mm) of PM with aerodynamic diameters < 2.5 μm ($PM_{2.5}$)

and aerodynamic diameters < 10 μm (PM_{10}) was collected for 24 h using a median-flow particle sampler (Tianhong, Wuhan, Co. Ltd) with a flow rate of 100 $L \cdot min^{-1}$. The dust quartz filter sample (P) from the coking plant chimney at S1 was collected three times in one day with a flow rate 16.67 L/min by diluting channel sampling equipment (made by Qingdao Laoshan Ltd., Qingdao, China), which was calibrated by a gas mass flow calibrator (API 700, New York, NY, USA).

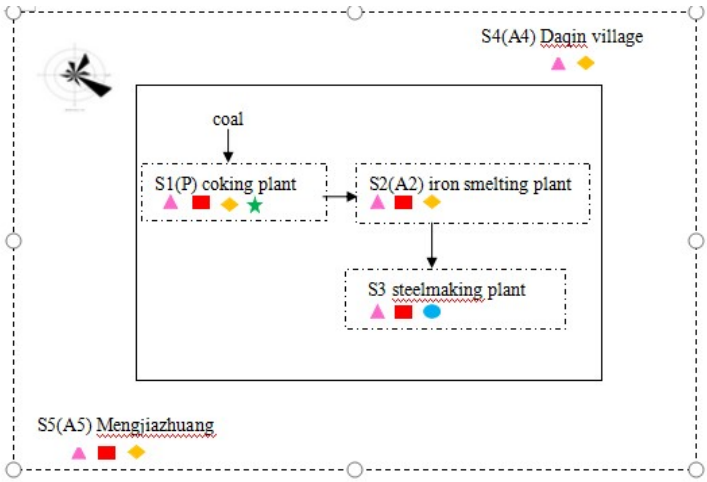

Note: ▲road dust; ■roof dust ; ●bare soil; ◆ atmospheric PM; ★coking plant flue dust

Fig. 1 Spatial distribution of the sampling sites

1.2 Sample pretreatment and instrumental analysis

Approximately 10 g of each dust sample and quartz filter sample, including the atmospheric PM filter samples and one dust particle sample from the coking plant chimney, was extracted for 16 h at 60 °C with n-hexane, using a set of soxhlet extractors. The extractant was concentrated to 2–3 mL by a rotary evaporator and then purified through a silica gel column. Then, the eluents were collected and concentrated to 0.5 mL, followed by dilution to 1 mL with n-hexane for the subsequent analysis.

The analysis of PAHs was performed with an electrospray ionization source in single reaction monitoring mode using gas chromatography mass spectrometry with a DB-5MS column (60 m × 0.25 mm × 0.25 μm; Agilent). The instrumental analysis conditions were set as the following: injection temperature of 250 °C, column flow velocity of 1.10 mL/min, split flow ratio of 10:1; column pressure of 69.3 kPa, oven temperature of 40 °C, and sample quantity of 1.0 μL.

The raising temperature program was listed as follows: initial temperature of 70 °C for 1 min; warming to 240 °C at a heating rate of 20 °C/min; and warming to 310 °C at a heating rate of 10 °C/min and maintained for 20 min. The carrier gas was high-purity nitrogen.

The target compounds for monitoring and analysis were 16 types of US EPA PAHs, and the specific substances and their properties, limit of detection, and limit of quantification were shown in Table 1.

1.3 Quality control

Among the 16 types of PAHs, only BaA, Chry, IcdP, and DahA were detected in the analytical blank samples, whereas others could not be detected within their limit of detection. The detected blank sample concentrations of BaA, Chry, IcdP, and DahA, were 0.0031, 0.0085, 0.0055, and 0.0067 μg/mL, respectively, indicating that no interference for the target compounds was present in the experiment (Li et al. 2015). These concentrations were subtracted from the concentrations in the actual samples to account for the blank contamination. At the time of detection, the standard solutions (2000 μg/mL, AccuStandard Inc., US) with

concentrations of 0.2, 0.4, 0.6, 0.8, 1.0, and 2.0 mg/L were configured, with correlation coefficients, R^2, all above 0.9997. Indicator pyrene was added to the blank sampling, and the recovery rate was between 82%–113% (meeting the EPA requirement 70%–130%), and the relative standard deviation (RSD) was 1.74%–12.6% (meeting the EPA requirement of RSD < 20%) (Li et al. 2015).

Table 1 Names and properties of 16 US EPA priority PAHs.

Serial number	Name	abbreviations	Number of benzene rings	limit of detection (μg/mL)	limit of quantification (μg/mL)
1	naphthalene	NaP	2	0.002	0.005
2	acenaphthene	Ace	3	0.004	0.01
3	acenaphthylene	Acy	3	0.005	0.012
4	fluorine	Flu	3	0.005	0.013
5	phenanthrene	Phe	3	0.003	0.008
6	anthracene	Ant	3	0.004	0.011
7	fluoranthene	Flua	4	0.007	0.124
8	pyrene	Pyr	4	0.004	0.013
9	benzo[a]anthracene	BaA	4	0.002	0.007
10	chrysene	Chry	4	0.007	0.013
11	benzo[*b*]fluoranthene	BbF	5	0.003	0.006
12	benzo[*k*]fluoranthene fluoranthene	BkF	5	0.004	0.013
13	benzo[a]pyrene	BaP	5	0.004	0.007
14	indeno [1,2,3 -*cd*] pyrene	IcdP	6	0.005	0.015
15	dibenz[ah]anthracene	DahA	5	0.006	0.013
16	benzo[ghi]perylene	BghiP	6	0.004	0.013

1.4 Particle Size Analysis Method

The laser particle size analyzer (LS-C(I), Zhuhai Omec Company, Zhuhai, China) was used to test the particle size distribution of two typical samples of road dust and roof dust. Before testing the size distribution, the dust particle samples were pretreated by 300 μm stainless steel sieve.

1.5 Risk assessment methods

The toxic equivalency value of BaP (TEQ_{BaP}) is used to evaluate the potential ecological risk caused by the PAHs (Cheng et al. 2005; Zhou et al. 2018). The calculation method is given in Eq.1.

$$TEQ_{Bap} = \sum (C_i \times TEF_i) \quad \text{(Eq.1)}$$

where C_i is the concentration of the i^{th} type of PAHs μg/g), TEF_i is the toxic equivalency factor of the i^{th} type of PAHs (Table 3), and TEQ_{BaP} is the BaP-based toxic equivalency value (μg/g) (Agarwal et al. 2009; Li et al. 2017).

The carcinogenic risk of PAHs to human health is manifested in three ways: direct ingestion, inhalation, and dermal contact (USEPA 2011). The effect of PAHs on human health is calculated according to the carcinogenic health risk assessment model recommended by the US EPA (USEPA 2002). The calculation formulas are listed as follows.

$$ILCR_{ing} = \frac{TEQ_{Bap} \times CSF_{ing} \times \sqrt[3]{BW/70} \times IR_{ing} \times EF \times ED}{BW \times AT \times 10^{6}} \quad \text{(Eq.2)}$$

$$ILCR_{inh} = \frac{TEQ_{Bap} \times CSF_{inh} \times \sqrt[3]{BW/70} \times IR_{inh} \times EF \times ED}{BW \times AT \times PEF} \quad \text{(Eq.3)}$$

$$ILCR_{derm} = \frac{TEQ_{Bap} \times CSF_{derm} \times \sqrt[3]{BW/70} \times SA \times SL \times ABS \times EF \times ED}{BW \times AT \times 10^{6}} \quad \text{(Eq.4)}$$

$$TILCR = ILCR_{ing} + ILCR_{inh} + ILCR_{derm} \quad \text{(Eq.5)}$$

In Eqs.2-5, $ILCR_{ing}$, $ILCR_{inh}$, and $ILCDR_{derm}$ are the carcinogenic health risk values of ingestion, inhalation, and skin contact, respectively. TILCR is the sum of the three carcinogenic health risks; IR_{ing} is the ingesting rate (mg/d); IR_{inh} is the inhalation rate (m^3/d), EF is the exposure frequency (d/a), ED is the exposure duration (a), BW is the body weight (kg), AT is the average exposure time (a), PEF is the particulate matter emission factor (m^3/kg); SL is the skin adhesion [mg/(cm^2·d)], SA is the exposed skin area (cm^2), ABS is the skin absorption factor; and CSF_{ing}, CSF_{inh}, and CSF_{derm} are the carcinogenic slope coefficients of the three exposure pathways, which are 7.3, 3.85, and 25.0, respectively (kg·d)/mg (Wang 2017). When ILCR or TILCR is below 10^{-6}, between 10^{-6} and 10^{-4}, or above 10^{-4}, this means that there is no carcinogenic risk, low to moderate carcinogenic risk, or high carcinogenic risk, respectively (Knafla et al. 2006).

2 Results and Discussion

16 US EPA priority PAH concentrations in road dust (RD), roof dust (RF), and bare soil (BS) at different sites were shown in Table 2.

Table 2 Concentration of PAHs (μg/g) in the RD, RF, and BS from five sites surrounding the ISE

PAHs	S1		S2		S3			S4	S5	
	RD	RF	RD	RF	BS	RD	RF	RD	RD	RF
NaP	0.730 ± 0.080	0.970 ± 0.092	0.160 ± 0.014	0.080 ± 0.071	0.990 ± 0.088	0.020 ± 0.018	0.070 ± 0.008	N.D.	0.060 ± 0.053	0.020 ± 0.002
Acy	1.610 ± 0.153	0.260 ± 0.025	0.02 ± 0.002	0.010 ± 0.001	0.040 ± 0.004	0.020 ± 0.002	0.010 ± 0.001	N.D.	0.010 ± 0.001	N.D.
Ace	0.140 ± 0.093	0.090 ± 0.008	0.02 ± 0.002	0.010 ± 0.001	0.100 ± 0.009	0.010 ± 0.001	0.010 ± 0.001	N.D.	0.010 ± 0.001	0.010 ± 0.001
Flu	0.730 ± 0.069	0.420 ± 0.040	0.09 ± 0.011	0.030 ± 0.027	0.150 ± 0.015	0.010 ± 0.001	0.010 ± 0.001	N.D.	0.050 ± 0.005	N.D.
Phe	3.570 ± 0.303	1.700 ± 0.162	0.21 ± 0.019	0.250 ± 0.024	1.070 ± 0.102	0.120 ± 0.012	0.230 ± 0.025	0.020 ± 0.002	0.290 ± 0.028	0.060 ± 0.007
Ant	1.440 ± 0.130	0.350 ± 0.040	0.040 ± 0.004	0.030 ± 0.004	0.080 ± 0.010	0.040 ± 0.005	0.020 ± 0.002	0.010 ± 0.001	0.050 ± 0.006	0.010 ± 0.001
Flua	4.620 ± 0.439	1.970 ± 0.213	0.130 ± 0.014	0.360 ± 0.032	1.310 ± 0.144	0.260 ± 0.025	0.470 ± 0.042	0.040 ± 0.004	0.260 ± 0.023	0.060 ± 0.006
Pyr	3.060 ± 0.127	1.250 ±0.113	0.120 ± 0.012	0.270 ± 0.020	1.130 ± 0.021	0.160 ± 0.014	0.260 ± 0.029	0.030 ± 0.004	0.330 ± 0.036	0.040 ± 0.005
BaA	3.350 ± 0.285	0.990 ±0.089	0.160 ± 0.018	1.730 ± 0.156	0.540 ± 0.049	0.180 ± 0.015	0.430 ± 0.041	0.050 ± 0.005	0.590 ± 0.053	0.080 ± 0.007
Chry	3.430 ± 0.307	1.820 ± 0.127	0.170 ± 0.015	1.900 ± 0.171	2.710 ± 0.300	0.330 ± 0.031	0.460 ± 0.044	0.050 ± 0.006	0.640 ± 0.061	0.080 ± 0.010
BbF	7.270 ± 0.118	2.280 ± 0.196	0.070 ± 0.008	0.580 ± 0.055	2.140 ± 0.311	0.360 ± 0.034	0.240 ± 0.023	0.060 ± 0.053	0.290 ± 0.025	0.070 ± 0.008
BkF	7.270 ± 0.121	2.280 ± 0.196	0.070 ± 0.008	0.580 ± 0.055	1.820 ± 0.164	0.360 ± 0.020	0.240 ± 0.021	0.060 ± 0.005	0.290 ± 0.021	0.070 ± 0.008
BaP	3.030 ± 0.118	0.880 ± 0.079	0.030 ± 0.003	0.210 ± 0.021	0.630 ± 0.069	0.120 ± 0.013	0.070 ± 0.006	0.040 ± 0.004	0.210 ± 0.019	0.040 ± 0.004
IcdP	2.730 ± 0.127	0.710 ± 0.067	0.030 ± 0.004	0.160 ± 0.017	0.410 ± 0.044	0.080 ± 0.071	0.050 ± 0.006	0.040 ± 0.004	0.120 ± 0.013	0.050 ± 0.007
DahA	1.190 ± 0.107	0.280 ± 0.025	0.030 ± 0.003	0.100 ± 0.009	0.170 ± 0.015	0.050 ± 0.044	0.030 ± 0.027	0.030 ± 0.002	0.100 ± 0.013	0.030 ± 0.004
BghiP	2.800 ± 0.122	0.890 ±0.080	0.030 ± 0.003	0.260 ± 0.023	0.700 ± 0.067	0.090 ± 0.080	0.060 ± 0.007	0.040 ± 0.004	0.210 ± 0.186	0.050 ± 0.005

$\sum_{16}$ PAHs	46.970 ± 4.791	17.140 ± 4.462	1.370 ± 0.117	6.550 ± 0.583	13.990 ± 1.203	2.210 ± 0.188	2.660 ± 0.246	0.460 ± 0.043	3.510 ± 0.325	0.670 ± 0.062

N,D. means not detected.

2.1 Concentration level of PAHs in dusts

2.1.1 Concentration level of PAHs in road dust

The total concentration of the 16 PAHs ($\sum_{16}$ PAHs) in the road dust samples ranged from (0.460 ± 0.043) to (46.970 ± 4.791) μg/g in Table 2, with an average value of (10.892 ± 1.185) μg/g. Among the five sampling sites, the highest $\sum_{16}$ PAHs value was found at S1, followed by S5 and S3, and the lowest values appeared at S4, upwind of the ISE. The S1 sampling site, located near the coking plant, had the highest PAHs concentration level. This phenomenon was consistent with conclusions from previous studies that showed that the sedimentation rate of PAHs near iron and steel works was much greater than that of the other zones (Amodio et al 2014; Yang et al. 2002). Moreover, the wind direction can significantly affect the PAH concentrations. The $\sum_{16}$ PAH concentration at S5, downwind of the ISE, was (3.510 ± 0.325) μg/g and was approximately 7 times the value at S4, upwind of the ISE. In addition, the individual PAH concentrations were all below 0.1 μg/g, suggesting that it can be affected by wind direction. Vasilakos et al. (2007) reported that both wind speed and wind direction had an effect on the PAHs concentrations with the source of the pollution coming from different directions.

The most abundant individual PAHs were BbF and BkF in the road dust samples at S1, S3, and S4. However, the dominant compounds were Phe and Chry at S2 and Chry and BaA at S5. Carcinogenic BaP was detected in all dust samples, and the BaP concentration at site S1 near the coking plant had a higher value than that at other sites. This indicated that the various production processes from the ISE could impact the surrounding environment (Liu et al. 2004).

Comparison with other reports shows that the average concentrations of PAHs in road dust near the ISE were similar, with a value of 10.62 μg/g in Xi'an (Wei et al. 2015), slightly higher than that in Shanghai and Sydney (Nguyen et al. 2014; Jia et al. 2017). Notably, in our study area, only the PAH concentration level at S1 was much higher than previously reported levels, and the concentrations at the other sampling sites were far below those reported in the literature. This suggested that industrial activities from the ISE were the sources of PAHs in the dust samples of Laiwu.

2.1.2 Concentration level of PAHs in roof dust

In Table 2, the total concentration of the 16 PAHs was between (0.670 ± 0.062) μg/g and (17.140 ± 4.462) μg/g in roof dust, with an average value of (6.751 ± 0.692) μg/g. The highest $\sum_{16}$ PAHs value was found at S1, followed by S2 (6.550 ± 0.583 μg/g) and S3 (2.660 ± 0.246 μg/g), and the lowest values appeared at S5. Because the S1 sampling site was located near the coking plant, the roof dust at this site had the highest PAH concentration. This phenomenon was in accordance with the level of $\sum_{16}$ PAHs in road dust at the S1 site (Table 2). As is known, PAHs are more readily generated during the incomplete combustion of fossil fuels in the coking process, especially in the absence of oxygen (Li et al. 2009). Moreover, the PAH with the highest concentration of roof dust differed at four sites, in which BbF and BkF, Chry, Flua, and BaA and Chry exhibited the highest roof dust concentrations at S1, S2, S3, and S5, respectively. Interestingly, the most abundant PAHs for roof dust and road dust at S1 were similar. There is little published data regarding the concentration of PAHs in roof dust; thus, our results are significant in providing some guidance on PAH pollution.

2.1.3 **Distribution of PAHs in dust with sampling height**

Road dust and roof dust at the same sample sites were collected from different heights, representing the surface ground (low height) and 10 m height above ground (high height). The distribution of PAHs in dust at different sampling heights was shown in

Fig. 2. The PAH concentrations were higher in roof dust than in road dust at S2 and S3, whereas they were higher in road dust at S1 and S5. The $\sum_{16}$ PAH level of road dust was almost 2.74 and 5.24 times higher than that of roof dust at S1 and S5, respectively; for example, BbF and BkF at S1 and BaA and Chry at S5 were significantly higher in road dust than in roof dust. Meanwhile, the $\sum_{16}$ PAH concentration of road dust was 0.21 and 0.82 times lower than that of roof dust at S2 and S3, respectively; for instance, BaA and Chry at S2 were remarkably higher in roof dust than in road dust. This is mainly because the combustion of coal in the coking plant at S1 was a dry distillation process; meanwhile, severe hypoxia and high temperatures in the furnace were conducive to the generation of PAHs. The dust on the roof is not only the receiver of PAHs discharged from the coking plant flue but also the secondary contributors to the road dust. Because of its complex sources, the order of PAH concentrations for the road dust and roof dust was different at the four sampling sites, mainly attributed to the influence of the different sampling sites and the distance to the different industrial processes of the ISE.

PAHs containing four or more rings were defined as high-ring PAHs, whereas others were considered to be low-ring PAHs (Adekunle et al. 2017). The ring distribution of PAHs in the dust samples are presented in Fig. 3. In this study, different PAH sources, such as road dust and roof dust, have a similar PAH ring distribution such that high-ring PAHs had a higher proportion than low-ring PAHs. Four-ring PAH concentrations were the highest in roof dust at S2 and S3, and road dust at S5, whereas PAHs with four and five rings were both abundant at the other sites, followed by PAHs with three rings. Moreover, high-ring PAHs were mainly present on the surface of the road dust, whereas low-ring PAHs were more likely to exist on roof dust. The abundance of three-to-five-ring PAHs in the dust indicated that the dusts were exposed for a long time to PAHs that originated from industrial activities in these areas.

Typical samples of roof dust and road dust were collected to illustrate their particle size distribution. As were shown in Fig. 4, road dust sample showed a skewed distribution and leaned toward larger particles, whereas roof dust sample exhibited a normal distribution. The peak of the particle size distribution of roof dust and road dust reached 46.13 μm and 80.46 μm, in which the maximum proportion was 8.50% and 8.91%, respectively. D_{10}-D_{90} in road dust (12.42-200.32 μm) was larger than that in roof dust (5.44-149.16 μm), which indicated the compositional complexity of road dust. The D_{50} of road dust (75.30 μm) was higher than that of roof dust (32.63 μm). The particle size of roof dust was finer, whereas the particle size of road dust was coarser.

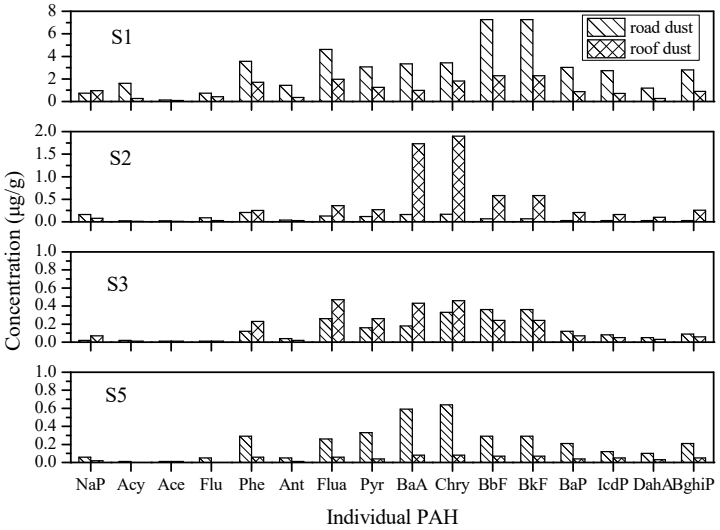

Fig. 2 Distribution of PAH of road dust and roof dust at various sampling sites

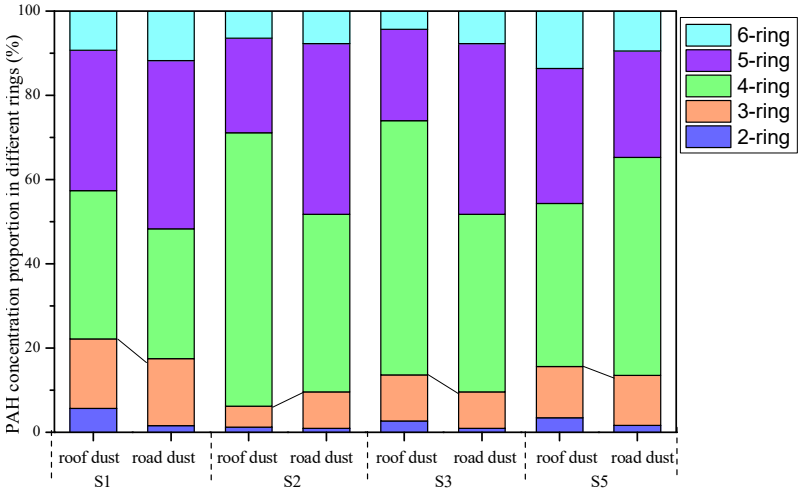

Fig. 3 Distribution of PAH with various rings at the sampling sites

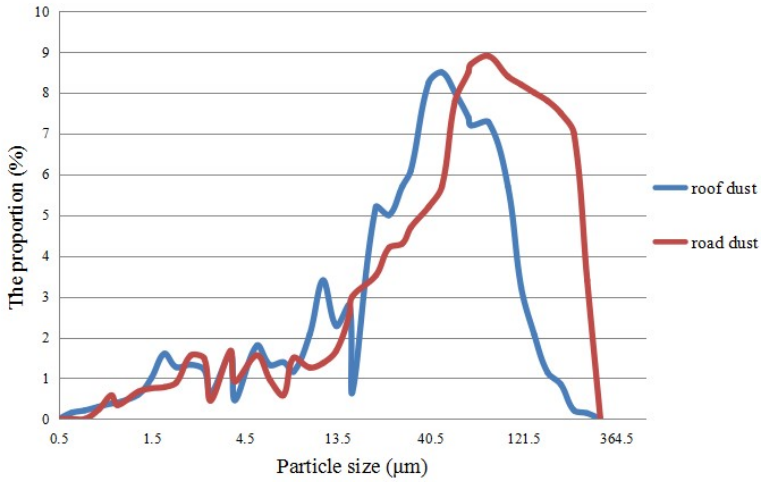

Fig. 4 Distribution of particle size in roof dust and road dust

2.1.4 Concentration level of PAHs in bare soil

The sampling site of bare soil in this study is located in the steelmaking plant (S3). The total concentration of PAHs (Σ_{16} PAHs) was 13.990 ± 1.203μg/g in bare soil (Table 2). Among these PAHs, Chry had the highest concentration (2.710 ± 0.300 μg/g), followed by BbF (2.140 ± 0.311μg/g) and BkF (1.820 ± 0.164 μg/g). The concentrations of Acy, Ant, Ace, and Flu were quite lower. Notably, the concentration of BaP, a carcinogenic PAH, was 0.630 ± 0.069 μg/g.

Currently, some reports are available concerning the concentration of PAHs in the soil surrounding steelmaking plants in China. Dong et al. (2016) found the concentrations of the sixteen PAHs to be between 0.02 and 20.06 μg/g (mean value of 2.56 μg/g), among which the BaP concentration was 0.16 μg/g in soil surrounding a steelmaking plant in northern China. However, Tian et al. (2013) reported a higher concentration of Σ_{16} PAHs and BaP of 32.10 and 0.58 μg/g, respectively, at another steelmaking plant located in northeastern China. Furthermore, the total concentration of these PAHs was up to 32.45 μg/g at a coking plant in Beijing (Feng et al. 2009). From these results, we found the concentration of PAHs of bare soil in our study to be

near an average level; it was below average around the steelmaking and coking plants in northeastern China and Beijing but above average near the steelmaking plant in northern China.

Chry is one of the carcinogenic PAHs from coal combustion (Harrison et al. 1996; Mastral et al. 1996). The Chry concentration was up to 2.710 ± 0.300 μg/g in our study, which was much higher than the previous reports of 1.57 μg/g (Hou and Zhang. 2012). There is no currently published evaluation standard for soil PAHs in China; thus, the Canadian soil quality benchmark was used to assess soil quality (Kong et al. 2018). The concentration of BaP was 0.630 ± 0.069 μg/g in the collected bare soil, which was higher than the reference value of 0.10 μg/g in agricultural soil. Thus, it was indicative of severe pollution in the bare soils in the tested regions.

In summary, different sampling areas contained different PAHs; however, the main types of PAHs in road dust, roof dust, and bare soil at the same sampling site were similar: BbF and BkF were the main pollutants in road and roof dust at S1; BaP and Chry were the main pollutants at S2; the main pollutants were Chry, BbF, and BkF in the bare soil, road dust, and roof dust at S3; the main pollutants were BbF and BkF from road dust at S4; and at S5, the main PAHs were BaP and Chry.

2.2 Impact of PAHs in dust on environment atmospheric PM

The $\sum_{16}$ PAHs concentration in $PM_{2.5}$ and $PM_{2.5-10}$ at atmospheric PM sites (A2, A4, A5) were shown in Fig. 5. The $\sum_{16}$ PAHs concentration was the highest at A2 inside the iron-smelting plant of the ISE, at 3.01 μg/m^3 in $PM_{2.5}$ and 0.58 μg/m^3 in $PM_{2.5-10}$, respectively, and the concentration of $\sum_{16}$ PAHs in A4, upwind of the ISE, was remarkably lower than that in A5, downwind of the ISE. This confirmed that the ISE had a heavy environmental impact on PAHs in the surrounding atmospheric PM, consistent with the research conclusions of related references (e.g., Cas et al. 2012). The mass concentration of $\sum_{16}$ PAHs in $PM_{2.5}$ was 9.741 μg/m^3 in the environmental air, approximately 1 km from a coking plant (Wang et al. 2013). The $\sum_{16}$ PAHs concentration in our collected samples was lower than that in the literature. The $\sum_{16}$ PAHs concentration proportion of $PM_{2.5}$ was 81.83% (A2), 83.84% (A4), and 94.49% (A5) of that in PM_{10}. Such a high proportion suggested that PAHs of finer particle size should be given significant emphasis.

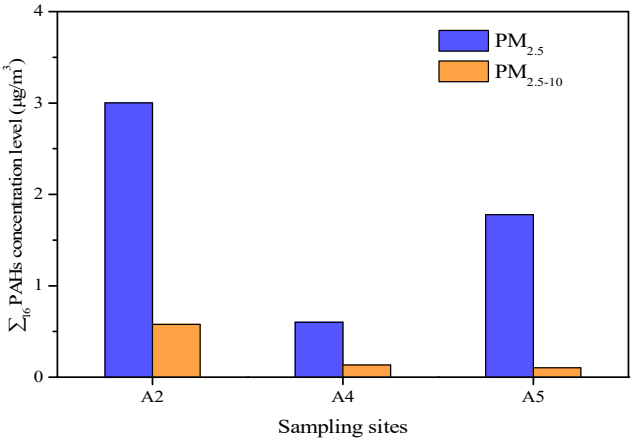

Fig. 5 $\sum_{16}$ PAHs concentrations in atmospheric particulate matter (PM), roof dust, and road dust at different sampling sites

To reflect the environment impact of individual PAHs from dusts on atmospheric PM, flue dust from one coking plant was collected to compare with the individual PAHs of roof dust and road dust by averaging the data from the different sites. As shown in Fig 6, road dust and roof dust exhibit similar concentration curves, in which BbF and BkF were the main components of roof dust and road dust, and the PAH with the highest concentration in road dust was Chry. BbF and BkF were also the dominant

individual PAHs of the flue dust, whereas the concentration of high-ring PAHs, including BaP, IcdP, DahA, and Behia, was also high. This could be explained as the PAHs with more rings underwent complex physical and chemical reactions in the atmosphere after being discharged from the flue dust, causing a transformation into other environment media. Shi et al. (2014) reported that high-ring PAHs were derived from the incomplete combustion of fossil fuels and more likely to be adsorbed onto the soil and dust particles (Duan et al. 2015). This might also explain the distribution of PAHs in the present study. For atmospheric $PM_{2.5}$, the concentration curves of the different sample sites were similar; the concentration of BbF was the highest, followed by Flua and BkF. Moreover, the concentration of BaP, a heavily carcinogenic PAH, was 0.50, 0.08, and 0.30 μg/m^3 in A2, A4, and A5, respectively, all exceeding the 2nd standard value of the National Ambient Air Quality Standard of BaP (0.0025 μg/m^3) in China. Furthermore, BaP/$\sum_{16}$ PAHs ranged from 7.03% to 9.62% in atmospheric $PM_{2.5}$ and from 4.44% to 6.28% in dusts. Hence, the higher BaP concentration and BaP/$\sum_{16}$ PAHs value suggested that atmospheric PAHs should be paid much more attention, as they may have a serious impact on the surrounding atmosphere.

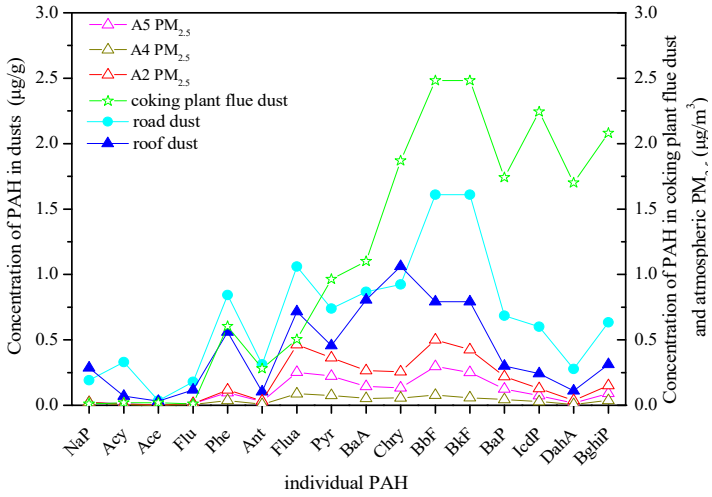

Fig. 6 Individual PAH concentrations in dust, coking plant, flue dust, and atmospheric $PM_{2.5}$

2.3 Probabilistic health risk assessment of PAHs

The toxic equivalent factors and equivalency values and the carcinogenic risk evaluation results of the 16 PAHs were listed in Table 3. The BaP-based toxic equivalency (TEQ_{BaP}) values exhibited great differences, depending on the sampling site. For example, the TEQ_{BaP} of the sixteen PAHs was the highest at S1, (1.823 ± 0.091)-(6.370 ± 0.306) μg/g, and it was (0.095 ± 0.008)-(0.638 ± 0.031) μg/g, (0.202 ± 0.017)-(1.330 ± 0.064) μg/g, 0.085 ± 0.004 μg/g, and (0.986 ± 0.009)-(0.443 ± 0.021) μg/g at S2, S3, S4, and S5, respectively (Table 2). The TEQ_{BaP} of the seven carcinogenic PAHs accounted for (93.760 ± 7.969)-(95.590 ± 8.125)% of the total TEQ_{Bap} of 16 PAHs, indicating that these carcinogenic PAHs led to the ecological risk. Among the seven carcinogenic PAHs, the health risk of BaP was the highest. The $\Sigma_{16}TEQ_{BaP}$ of the various dust samples followed the order: road dust at S1 (6.370 ± 0.306 μg/g) > roof dust at S1 (1.823 ± 0.091 μg/g) > bare soil at S3 (1.330 ± 0.064 μg/g) > roof dust at S2 (0.638 ± 0.031 μg/g) > road dust at S5 (0.443 ± 0.021 μg/g) > road dust at S3 (0.272 ± 0.013 μg/g) > roof dust at S4 (0.202 ± 0.017μg/g) > roof dust at S5 (0.099 ± 0.009 μg/g) > road dust at S2 (0.096 ± 0.008 μg/g) > road dust at S4 (0.085±0.004 μg/g). Evidently, S1 demonstrated the highest $\Sigma_{16}TEQ_{BaP}$. Among the various dust samples, the $\Sigma_{16}TEQ_{BaP}$ values were higher in road dust than that in roof dust, with the exception of that at S2.

Presently, there are few reports on the TEQs of PAHs in dust samples. Taking that into consideration, a rough comparison was made regarding the TEQs of PAHs in soils from the different sampling sites in and around an ISE, which showed that the $\Sigma_{16}TEQ_{BaP}$ and $\Sigma_{7}TEQ_{BaP}$ were 0.340 and 0.330 μg/g, respectively, and the $\Sigma_{7}TEQ_{BaP}$ to $\Sigma 16TEQ_{BaP}$ ranged from 76.400% to 99.100% (Tao et al. 2016). These findings indicated that carcinogenic PAHs were the main contributors to the total TEQ_{BaP}. Moreover, the concentration of carcinogenic PAHs in our study was higher than that reported in the literature (Tao et al. 2016), suggesting a heavier potential ecological risk for these carcinogenic PAHs in the investigated regions.

Carcinogenic risk evaluation results of the PAHs in road dust, roof dust, and bare soil inside the ISE and in the surrounding environment were listed in Table 4. The ranges of TILCR for children, adult males, and adult females were $(1.061 \pm 0.171) \times 10^{-5}$ - $(7.915 \pm 0.579) \times 10^{-4}$, $(8.274 \pm 0.793) \times 10^{-6}$ - $(6.175 \pm 0.601) \times 10^{-4}$, and $(7.486 \pm 0.649) \times 10^{-6}$ - $(5.587 \pm 0.512) \times 10^{-4}$, respectively. Road dust exhibited heavier carcinogenic risk than roof dust, and the TILCR of bare soil at S3 was higher than that of road dust and roof dust, indicating potentially heavier pollution in bare soil. Among the different exposure pathways, the order of the carcinogenic risk value was $ILCR_{derm} > ILCR_{ing} > ILCR_{inh}$. $ILCR_{inh}$ did not indicate any carcinogenic risk as the value was lower than 10^{-6}. $ILCE_{ing}$ in road and roof dust at S1, roof dust at S2, and bare soil at S2 were between 10^{-6} and 10^{-4}, suggesting a low to moderate risk of carcinogenesis, and LCE_{derm} of road and roof dust at S1 and bare soil at S2 exceeded 10^{-4}, indicating a higher carcinogenesis risk. For different age groups, $ILCR_{ing}$ and IL_{CRinh} in adults were higher than in children, whereas the $ILCR_{derm}$ value for children was slightly higher than that for adults, indicating that the carcinogenesis risk was increasing with age, but children was easily to suffer from skin contact. Moreover, male $ILCR_{inh}$ and $ILCR_{derm}$ was higher than female, while male $ILCR_{ing}$ was lower than that of female, mainly because of the female lower respiratory rate, lower weight, lower skin contact area, and longer lifetime (Knafla et al. 2006).

Table 3 Health risk caused by PAHs in RD, RF, and BS inside the ISE and in the surrounding environment based on the TEQ_{BaP} ($\times 10^{-3}$ μg/g)

PAH	TEF	S1		S2		S3			S4	S5	
		Rd	Rf	Rd	Rf	Bs	Rd	Rf	Rd	Rd	Rf
NaP	0.001	0.728 ± 0.061	0.970 ± 0.077	0.155 ± 0.017	0.080 ± 0.010	0.992 ± 0.011	0.020 ± 0.002	0.070 ± 0.008	N.D.	0.057 ± 0.007	0.020 ± 0.002
Acy	0.001	1.611 ± 0.128	0.260 ± 0.020	0.016 ± 0.001	0.010 ± 0.010	0.043 ± 0.046	0.016 ± 0.002	0.010 ± 0.001	N.D.	0.010 ± 0.001	N.D.
Ace	0.001	0.136 ± 0.010	0.090 ± 0.010	0.023 ± 0.002	0.010 ± 0.197	0.103 ± 0.185	0.006 ± 0.001	0.010 ± 0.001	N.D.	0.012 ± 0.001	0.010 ± 0.001
Flu	0.001	0.731 ± 0.057	0.420 ± 0.033	0.094 ± 0.007	0.030 ± 0.406	0.148 ± 0.082	0.013 ± 0.001	0.010 ± 0.001	N.D.	0.054 ± 0.006	N.D.
Phe	0.001	3.573 ± 0.278	1.700 ± 0.144	0.208 ± 0.016	0.250 ± 0.026	1.073 ± 0.091	0.120 ± 0.014	0.230 ± 0.018	0.024 ± 0.003	0.290 ± 0.025	0.060 ± 0.006
Ant	0.01	14.350 ± 1.119	3.500 ± 0.273	0.380 ± 0.030	0.300 ± 0.026	0.750 ± 0.064	0.350 ± 0.030	0.200 ± 0.017	0.070 ± 0.008	0.510 ± 0.043	0.100 ± 0.010
Flua	0.001	4.618 ± 0.360	1.970 ± 0.167	0.130 ± 0.011	0.360 ± 0.031	1.307 ± 0.111	0.261 ± 0.022	0.470 ± 0.040	0.035 ± 0.004	0.260 ± 0.022	0.060 ± 0.006
Pyr	0.001	3.064 ± 0.238	1.250 ± 0.106	0.115 ± 0.009	0.270 ± 0.023	1.128 ± 0.096	0.158 ± 0.013	0.260 ± 0.022	0.032 ± 0.004	0.326 ± 0.028	0.040 ± 0.004
BaA*	0.1	334.700 ± 24.098	99.000 ± 7.722	16.300 ± 1.271	173.000 ± 13.494	53.460 ± 4.170	18.300 ± 1.427	43.000 ± 3.354	5.100 ± 0.434	59.100 ± 4.610	8.000 ± 0.816
Chry*	0.01	34.330 ± 2.677	18.200 ± 0.873	1.680 ± 0.131	19.000 ± 1.520	27.107 ± 2.006	3.250 ± 0.241	4.600 ± 0.340	0.510 ± 0.043	6.400 ± 0.544	0.800 ± 0.082
BbF*	0.1	727.300 ± 52.365	228.000 ± 17.432	6.500 ± 0.507	58.000 ± 4.524	214.17 ± 16.705	36.200 ± 2.824	24.000 ± 2.864	5.700 ± 0.422	29.200 ± 2.278	7.000 ± 0.595
BkF*	0.1	727.300 ± 53.820	228.00 ± 17.784	6.500 ± 0.533	58.000 ± 4.526	181.515 ± 14.158	36.200 ± 2.823	24.000 ± 1.872	5.700 ± 0.445	29.200 ± 1.119	7.000 ± 0.574
BaP*	1	3026.000 ± 217.872	880.000 ± 63.361	33.000 ± 2.574	210.000 ± 16.382	631.500 ± 46.731	121.000 ± 9.438	70.000 ± 5.460	37.000 ± 2.886	207.000 ± 14.904	40.000 ± 3.120
IcdP*	0.1	272.600 ± 21.262	71.000 ± 4.899	3.300 ± 0.227	16.000 ± 1.248	41.445 ± 3.233	8.300 ± 0.647	5.000 ± 0.425	3.800 ± 0.262	11.900 ± 0.928	5.000 ± 0.370
DahA*	1	1191.000 ± 88.134	280.000 ± 20.162	27.000 ± 2.106	100.000 ± 6.900	169.200 ± 13.198	47.000 ± 3.666	30.000 ± 2.340	27.000 ± 2.106	97.000 ± 7.566	30.000 ± 2.340
BghiP	0.01	28.000 ± 1.932	8.900 ± 0.614	0.340 ± 0.039	2.600 ± 0.299	6.948 ± 0.514	0.870 ± 0.102	0.600 ± 0.069	0.380 ± 0.044	2.130 ± 0.245	0.500 ± 0.058
$\sum_{16}$ TEQ_{BaP}	/	6370.041 ± 305.761	1823.260 ± 91.163	95.741 ± 8.329	637.910 ± 30.621	1330.887 ± 63.883	272.06 ± 13.059	202.460 ± 17.209	85.351 ± 4.097	443.449± 21.286	98.590 ± 8.577
$\sum_{7}$ TEQ_{BaP}	/	6038.920 ± 271.751	1725.870 ± 82.841	89.770 ± 7.630	601.960 ± 28.894	1258.100 ± 56.615	259.830 ± 12.472	192.070 ± 9.219	80.920 ± 3.884	423.890 ± 20.347	92.560 ± 7.868
$\sum_{7}$TEQ/ $\sum_{16}$TEQ(%)	/	94.800 ± 7.204	94.660 ± 8.235	93.760 ± 7.969	94.360 ± 8.209	94.530 ± 8.035	95.500 ± 8.309	94.870 ± 8.064	94.800 ± 8.248	95.590 ± 8.125	93.880 ± 8.168

N.D. stands for none detected; PAHs with * refers to carcinogenic PAHs.

Table 4 Carcinogenic risk evaluation results of the PAHs in RD, RF, and BS inside the ISE and in the surrounding environment

Exposure	Age	S1		S2		S3			S4	S5	
		Rd	Rf	Rd	Rf	Bs	Rd	Rf	Rd	Rd	Rf
$ILCR_{ing}$	child	$(8.065 \pm 0.061) \times 10^{-6}$	$(2.308 \pm 0.103) \times 10^{-6}$	$(1.212 \pm 0.227) \times 10^{-7}$	$(8.079 \pm 0.598) \times 10^{-7}$	$(1.685 \pm 0.203) \times 10^{-6}$	$(3.444 \pm 0.149) \times 10^{-7}$	$(2.563 \pm 0.149) \times 10^{-7}$	$(1.081 \pm 0.193) \times 10^{-7}$	$(5.614 \pm 0.429) \times 10^{-7}$	$(1.248 \pm 0.119) \times 10^{-7}$
	Adult(male)	$(1.144 \pm 0.125) \times 10^{-6}$	$(3.274 \pm 0.135) \times 10^{-6}$	$(1.719 \pm 0.155) \times 10^{-7}$	$(1.146 \pm 0.149) \times 10^{-6}$	$(2.390 \pm 0.149) \times 10^{-6}$	$(4.886 \pm 0.444) \times 10^{-7}$	$(3.636 \pm 0.149) \times 10^{-7}$	$(1.553 \pm 0.413) \times 10^{-7}$	$(7.964 \pm 0.966) \times 10^{-7}$	$(1.771 \pm 0.416)) \times 10^{-7}$

	Adult(female)	$(1.170 \pm 0.109) \times 10^{-6}$	$(3.349 \pm 0.444) \times 10^{-6}$	$(1.759 \pm 0.163) \times 10^{-7}$	$(1.172 \pm 0.103) \times 10^{-6}$	$(2.445 \pm 0.249) \times 10^{-6}$	$(4.998 \pm 0.324) \times 10^{-7}$	$(3.719 \pm 0.149) \times 10^{-7}$	$(1.568 \pm 0.416) \times 10^{-7}$	$(8.146 \pm 0.973) \times 10^{-7}$	$(1.811 \pm 1.216) \times 10^{-7}$
$ILCR_{inh}$	child	$(3.753 \pm 0.023) \times 10^{-10}$	$(1.074 \pm 0.498) \times 10^{-10}$	$(5.641 \pm 0.438) \times 10^{-12}$	$(3.758 \pm 0.211) \times 10^{-11}$	$(7.841 \pm 0.644) \times 10^{-11}$	$(1.603 \pm 0.144) \times 10^{-11}$	$(1.193 \pm 0.197) \times 10^{-11}$	$(5.028 \pm 0.1) \times 10^{-12}$	$(2.613 \pm 0.259) \times 10^{-11}$	$(5.808 \pm 0.318) \times 10^{-12}$
	Adult(male)	$(1.570 \pm 0.149) \times 10^{-9}$	$(4.495 \pm 0.416) \times 10^{-10}$	$(2.360 \pm 0.219) \times 10^{-11}$	$(1.573 \pm 0.149) \times 10^{-10}$	$(3.281 \pm 0.119) \times 10^{-10}$	$(6.707 \pm 0.179) \times 10^{-11}$	$(4.991 \pm 0.497)) \times 10^{-11}$	$(2.104 \pm 0.149) \times 10^{-11}$	$(1.093 \pm 0.106) \times 10^{-10}$	$(2.431 \pm 0.201) \times 10^{-12}$
	Adult(female)	$(1.316 \pm 0.135) \times 10^{-10}$	$(3.767 \pm 0.355) \times 10^{-10}$	$(1.978 \pm 0.187) \times 10^{-11}$	$(1.318 \pm 0.216) \times 10^{-10}$	$(2.749 \pm 0.222) \times 10^{-10}$	$(5.621 \pm 0.981) \times 10^{-11}$	$(4.183 \pm 0.416) \times 10^{-11}$	$(1.763 \pm 0.144) \times 10^{-11}$	$(9.161 \pm 0.519) \times 10^{-11}$	$(2.037 \pm 0.106) \times 10^{-11}$
$ILCR_{derm}$	child	$(7.834 \pm 0.169) \times 10^{-4}$	$(2.242 \pm 0.178) \times 10^{-4}$	$(1.177 \pm 0.198) \times 10^{-5}$	$(6.069 \pm 0.597) \times 10^{-5}$	$(1.637 \pm 0.139) \times 10^{-4}$	$(3.346 \pm 0.961) \times 10^{-5}$	$(2.490 \pm 0.144) \times 10^{-5}$	$(1.050 \pm 0.077) \times 10^{-5}$	$(5.454 \pm 0.444) \times 10^{-5}$	$(1.213 \pm 0.198) \times 10^{-5}$
	Adult(male)	$(6.061 \pm 0.249) \times 10^{-4}$	$(1.735 \pm 0.198) \times 10^{-4}$	$(9.109 \pm 0.776) \times 10^{-6}$	$(5.478 \pm 0.446) \times 10^{-5}$	$(1.266 \pm 0.149) \times 10^{-4}$	$(2.588 \pm 0.931) \times 10^{-5}$	$(1.926 \pm 0.179) \times 10^{-5}$	$(8.120 \pm 0.498) \times 10^{-6}$	$(4.219 \pm 0.419) \times 10^{-5}$	$(9.380 \pm 0.799) \times 10^{-6}$
	Adult(female)	$(5.470 \pm 0.498) \times 10^{-4}$	$(1.566 \pm 0.149) \times 10^{-4}$	$(8.222 \pm 0.597) \times 10^{-6}$	$(7.926 \pm 0.497) \times 10^{-5}$	$(1.143 \pm 0.138) \times 10^{-4}$	$(2.336 \pm 0.138) \times 10^{-5}$	$(1.739 \pm 0.149) \times 10^{-5}$	$(7.329 \pm 0.619) \times 10^{-6}$	$(3.808 \pm 0.315) \times 10^{-5}$	$(8.466 \pm 0.777) \times 10^{-6}$
TILCR	child	$(7.915 \pm 0.579) \times 10^{-4}$	$(2.265 \pm 0.179) \times 10^{-4}$	$(1.190 \pm 0.295) \times 10^{-5}$	$(7.926 \pm 0.597) \times 10^{-5}$	$(1.654 \pm 0.113) \times 10^{-4}$	$(3.380 \pm 0.213) \times 10^{-5}$	$(2.516 \pm 0.188) \times 10^{-5}$	$(1.061 \pm 0.171) \times 10^{-5}$	$(5.510 \pm 0.444) \times 10^{-5}$	$(1.225 \pm 0.122) \times 10^{-5}$
	Adult(male)	$(6.175 \pm 0.601) \times 10^{-4}$	$(1.767 \pm 0.169) \times 10^{-4}$	$(9.281 \pm 0.479) \times 10^{-6}$	$(6.184 \pm 0.588) \times 10^{-5}$	$(1.290 \pm 0.143) \times 10^{-4}$	$(2.637 \pm 0.167) \times 10^{-5}$	$(1.963 \pm 0.179) \times 10^{-5}$	$(8.274 \pm 0.793) \times 10^{-6}$	$(4.299 \pm 0.416) \times 10^{-5}$	$(9.557 \pm 0.792) \times 10^{-6}$
	Adult(female)	$(5.587 \pm 0.512) \times 10^{-4}$	$(1.599 \pm 0.167) \times 10^{-4}$	$(8.398 \pm 0.761) \times 10^{-6}$	$(5.595 \pm 0.497) \times 10^{-5}$	$(1.167 \pm 0.112) \times 10^{-4}$	$(2.386 \pm 0.149) \times 10^{-5}$	$(1.776 \pm 0.159) \times 10^{-5}$	$(7.486 \pm 0.649) \times 10^{-6}$	$(3.890 \pm 0.349) \times 10^{-5}$	$(8.647 \pm 0.798) \times 10^{-6}$

3 Conclusions

To investigate the concentration levels of 16 priority PAHs in road dust and in roof dust inside and in the surrounding region of the ISE and its impact on atmospheric PM, dust and environment PM samples were collected. The results showed that PAH concentrations displayed great variability in dusts. The $\sum_{16}$ PAHs concentrations (in dry weight) were between 0.460 and 46.970 μg/g (avg ± sd: 10.892 ± 1.185 μg/g) in road dust, between 0.670 and 17.140 μg/g (avg ± sd: 6.751 ± 0.692 μg/g) in roof dust, and 13.990±1.203 μg/g in bare soil. Particle size distribution and PAH distribution of dust samples showed that road dust at low height had a coarser particle size and easily adsorbed high-ring PAHs (PAHs containing four or more rings). For atmospheric PM sites, $\sum_{16}$ PAHs was the highest inside the ISE, followed by sites downwind of the ISE, and the lowest at sites upwind of the ISE. This indicates a greater impact of dust on the atmospheric PM near the ISE. A similar concentration curve was synchronously observed, whereby the most abundant individual PAHs were BbF, Flua, and BkF at atmospheric PM sites and BbF, Chry, and BkF in dusts. BaP/$\sum_{16}$ PAHs ranged from 7.03% to 9.62% in atmospheric PM and ranged from 4.44% to 6.28% in dusts, suggesting that PAHs of atmospheric PM should be paid sufficient attention as they may have serious impact on the surrounding atmosphere.

Toxicity analysis revealed that PAHs with four rings, including carcinogenic PAHs, were the dominant pollutants in the studied area, and the $\Sigma_7 TEQ_{BaP}$ to $\Sigma_{16} TEQ_{BaP}$ ratio ranged from 76.400% to 99.100%. Based on the carcinogenic health risk assessment model recommended by the US EPA, the calculated results showed that skin contact with PAHs was the greatest health risk, followed by ingestion and inhalation. By comparison, road dust presented a greater carcinogenic risk than roof dust, while bare soil may suffer from heavier pollution. Meanwhile, the PAH carcinogenic risk of adults by skin contact and inhalation was higher than that of a child, and male PAH carcinogenic risk was higher than that of female.

Acknowledgements

This work was sponsored by the Science and Technology Development Project of Shandong Province (2014GSF117002).

References

Adekunle AS, Oyekunle JAO, Ojo OS et al(2017) Determination of polycyclic aromatic hydrocarbon levels of groundwater in Ife north local government area of Osun state, Nigeria.Toxicology Reports, 4:39-48.

Agarwal T, Khillare PS, Shridha V et al(2009) Pattern, sources and toxic potential of PAHs in the agricultural soils of Delhi, India. J Hazard Mater. 163:1033-1039.

Amodio M , Andriani E, Dambruoso P R et al (2013) A monitoring strategy to assess the fugitive emission from a steel plant. Atmos Environ, 79: 455-461.

Castro J, Berrojalbiz N, Wollgast J et al (2012) Polycyclic Aromatic Hydrocarbons (PAHs) in the Mediterranean Sea: Atmospheric Occurrence, Deposition and Decoupling with Settling Fluxes in the Water Column. Environ Pollut 166:40–47.

Cetin B, Yatkin S, Bayram A et al (2007) Ambient concentrations and source apportionment of PCBs and trace elements around an industrial area in Izmir, Turkey. Chemosphere, 69:1267-1277.

Chang KF, Fang GC, Chen JC et al (2006) Atmospheric polycyclic aromatic hydrocarbons (PAHs) in Asia: A review from 1999 to 2004. Environ Pollut, 142:390-396.

Cheng GE, Qiong AN, Dong YH (2005)Residue and risk assessment of polycyclic aromatic hydrocarbons (PAHs) in soils around a steel mill. J Eco Rural Environ ,21:66-66.

Christophe V, Khalil H, Christine DB, Patrick G(2006) Removal of polycyclic aromatic hydrocarbons from aged-contaminated soil using cyclodextrins, experimental study. Environ Pollut, 140:427-435.

Dong J, Huang Y, Li YX et al (2016) Pollution Characteristics and Health Risk Assessment of Polycyclic Aromatic Hydrocarbons in the Surface Soils of a Large Steel enterprise in the North of China.J Environ Sci China ,37:3540-3546.

Duan YH, Shen GF, Shu T, et al (2015) Characteristics of polycyclic aromatic hydrocarbons in agricultural soils at a typical coke production base in Shanxi, China. Chemosphere, 127: 64-69.

Feng, L,Yonggang L, Zhao Y et al (2015) Assessment on health risk of polycyclic aromatic hydrocarbons in airborne $PM_{2.5}$ in Tianjin.Pract Prev Med, 22,1322-1325.

Feng Y, Lu YL, Jia WT et al 2009). Distribution and Risk of Polycyclic Aromatic Hydrocarbons in Soils from Different Workshops of an Abandoned Coking Factory in Beijing. Asian J Ecotoxicol, l4:399-407.

Filho C. M. C., Bueno P. V. A. et. al (2020) Uncommon Sorption Mechanism of Aromatic Compounds onto Poly(Vinyl Alcohol)/Chitosan/Maleic Anhydride-ββ-Cyclodextrin Hydrogels, Plolymers,12(877):1-23.

Gang C, Xiaoy Z, Jianhui W (2015) Source apportionment and toxicity quantitation of PM2. 5-associated polycyclic aromatic hydrocarbons obtained from Chengdu，China．China Environ Sci,35:3150-3156．

Gilio AD, Ventrella G, Giungato P et al (2017) An intensive monitoring campaign of PAHs for assessing the impact of a steel plant. Chemosphere, 168: 171-182.

Harrison RM, Smith DJT, Luhana L (1996) Source apportionment of atmospheric polycyclic aromatic hydrocarbons collected from an urban location in Birmingham, UK. Environ Sci Techno,30:825-832.

He FP, Zhang ZH, Wan YY et al (2009) . Polycyclic aromatic hydrocarbons in soils of Beijing and Tianjin region, Vertical distribution, correlation with TOC and transport mechanism. J Environ Sci,21:675-685.

Hou YW, Zhang YC(2012) Characteristics and risk analysis of PAHs pollution in surface soil of a steel plant in fujian province, Environ Chemis ,31:1542-1548.

Huang XF, He LY, Hu M et al 2006) Annual variation of particulate organic compounds in PM_(2.5) in the urban atmosphere of Beijing. Atmos environ,40:2449-2458.

Jia JP, Bi CJ, Xue G et al .(2017) Characteristics, identification, and potential risk of polycyclic aromatic hydrocarbons in road dusts and agricultural soils from industrial sites in Shanghai, China. Environ Sci Pollut Res, 24:605-615.

Jiabao H,Shuxian F, Qingzi M (2014) Polycyclic aromatic hydrocarbons(PAHs) associated with fine particulate matters in Nanjing，China: distributions, sources and meteorological influences．Atmos Environ, 89: 207-215．

Knafla A,Phillipps KA,Brecher RW (2006) Development of a dermal cancer slope factor for benzopyrene. Regul Toxicol Pharm,45, 159-168．

Kong LL, Shi M.J, Liang Jet al (2018). Concentration and origin of polycyclic aromatic hydrocarbons in the soil of Dagang Oil Field. Environ Sci Techno,41:159-165.

Kuan L, Jiabin L, Chang Y et al (2018) Characteristics and source apportionment of polycyclic aromatic hydrocarbons in atmospheric $PM_{2.5}$ of Wuhan City, China．Res Enviro Sci, 31: 648-656．

Kulkarni P, Venkataraman C (2000) Atmospheric polycyclic aromatic hydrocarbons in Mumbai, India. Atmos Environ, 34:2785-2790.

Kwon HO, Choi SD (2014) Polycyclic aromatic hydrocarbons (PAHs) in soils from a multi-industrial city, South Korea. Sci Total Environ, 470-471:1494-1501.

Lan WS, He CF, Hang ZY, et al (2005)Pollution Characterization and Source Identification and Apportionment of Polycyclic Aromatic Hydrocarbons (PAHs) in Airborne Particulates. Res Environ Sci, 18:18-24.

Li, Y.X., Liu, Y., Wang, W.G., Dong, J., Wang, N., Gao, F.W. (2017). Concentration characteristic and ecological risk assessment of polycyclic aromatic hydrocarbons in the surface soils of a steel plant. Environ Chemis, 36:1320-1327.

Liu, D.M., Wang, W., Li, Y.Y. (2004). Distribution and occurrence of polycyclic aromatic hydrocarbons from the Shougang coking plant. Acta Sci Circums, 24: 746-749.

Liu GR, Shi GL, Zhang P et al (2014)Source identification and toxicity assessment of polycyclic aromatic hydrocarbons in particulate matter of Chengdu, China. China Environ Sci, 34:2479-2484.

Liu GR, Zheng MH, Liu WB et al (2009) Atmospheric emission of PCDD/Fs,PCBs, hexachlorobenzene, and pentachlorobenzene from the coking industry. Environ Sci Techno, 43: 9196-9201.

Mao IF, Chen CN, Lin YC et al (2007) Airborne particle PM2.5/PM10 mass distribution and particle-bound PAH concentrations near a medical waste incinerator. Atmos Environ, 41:2467-2475.

Mastral AM, Callén M, Murillo R(1996) Assessment of PAH emissions as a function of coal combustion variables. Fuel, 75:1533-1536

Mastral AM, Callén MS(2000)A Review on Polycyclic Aromatic Hydrocarbon (PAH) Emissions from Energy Generation. Environ Sci Techno, 34:66.

Mei Z, Caiqing Yan, Qiaoyun Y et al (2014) Characteristics of personal exposure to polycyclic aromatic hydrocarbons in public transportation environments in Beijing. Res Environ Sci,27:965-974．

Nguyen TC, Loganathan P, Nguyen TV et al (2014). Polycyclic aromatic hydrocarbons in road-deposited sediments, water sediments, and soils in Sydney, Australia: Comparisons of concentration distribution, sources and potential toxicity. Ecotoxicolenviron saf,104:339-348.

Odabasi M, Bayram A, Elbir T et al (2009) Electric Arc Furnaces for SteelMaking: Hot Spots for Persistent Organic Pollutants. Environ Sci Techno, 43:5205-5211.

Shi BF, Wu QL, Ouyang HX et al (2014) Characteristics and sources of polycyclic aromatic hydrocarbons in surface soil from industrial areas of Baise, Guangxi. China Environ Sci, 34:2593-2601.

Shi BF, Wu QL, Ouyang HX et al (2014)Characteristics and sources of polycyclic aromatic hydrocarbons in surface soil from industrial areas of Baise, Guangxi. China Environ Sci, 34:2593-2601.

Sun P, Basu I, Hites RA(2006)Temporal trends of polychlorinated biphenyls in precipitation and air at Chicago. Environ Sci Techno, 40: 1178-1183.

Takeshi O(2018) Spatial distribution and exposure risks of ambient chlorinated polycyclic aromatic hydrocarbons in Tokyo Bay area and network approach to source impacts. Environ pollut,232:267-274.

Tao SY, Ma J, Zhou YZ et al (2016)Polycyclic aromatic hydrocarbons pollution region in soils of typical coal-fired pollution region in Shanxi Province. Eco Sci, 25:2005-2013.

Tian J, Zhu YY, Yang HB et al (2013) Investigation, evaluation and source analysis of PAHs pollution in large steel mills and surrounding soils . Environ Chemis, 32: 1002-1008.

Tsai JH, Lin KH, Chen CY et al (2007)Chemical Constituents in Particulate Emissions from an Integrated Iron and Steel Facility. J Hazard Mater,147:111–119.

Tsapakis M, Stephanou EG (2015) Occurrence of gaseous and particulate polycyclic aromatic hydrocarbons in the urban atmosphere, study of sources and ambient temperature effect on the gas/particle concentration and distribution. Environ Pollut, 133:147-156.

USEPA (2002).Supplemental guidance for developing soil screening levels for superfund sites[R].Washington, DC: Office of Emergency and Remedial Response,3:68.-72．

USEPA. (2011).Exposure factors handbook [R]．EPA /600 /P- 95 / 002Fa.Washington，DC: USEPA,4:96-103.

Vasilakos C, Levi N, Maggos T et al (2007)Gas–particle concentration and characterization of sources of PAHs in the atmosphere of a suburban area in athens, greece. J Hazar Mater, 140:5-51.

Wang Z (2007)Regional study on soil polycyclic aromatic hydrocarbons in Liaoning: patterns，sources and cancer risks [D]. Dalian University of Technology, 15-69.

Wang J, Zhu LZ, Shen XY(2003) PAHs Pollution in Air of Coke Plant and Health Risk Assessment. Environ Sci , 24:135–138.

Wang H (2014). Current situation of prevention and control of key smoke and dust pollution sources in iron and steel industry. Chinese Society For Environm Sci,3:50-52.

Wei C, Han YM, Bandowe BAM et al (2015). Occurrence, gas/particle partitioning and carcinogenic risk of polycyclic aromatic hydrocarbons and their oxygen and nitrogen containing derivatives in Xi'an, central China. Sci Total Environ, 505: 814-822.

Wu YY (2015) Study on health risk assessment and management methods of persistent organic pollutants in coking industry .Taiyuan University of Science & Technology, 3: 40-50.

Yang HH, Lai SO, Hsieh LT et al (2002). Profiles of PAH Emission from Steel and Iron Industries. Chemosphere ,48:1061–1074.

Yinghong L,Zhiguo L, Jihua T et al (2016)Pollutional Characteristics and Sources Analysis of Polycyclic Aromatic Hydrocarbons in Atmospheric Fine Particulate Matter in Lanzhou City.Environ Sci, 37:2429-2431.

Sun Y M, Chen C Ding C et al (2019). Distribution Pattern, Emission Characteristics, and Environmental Impact of Polycyclic Aromatic Hydrocarbons (PAHs) in Download Ash and Dust from Iron and Steel Enterprise. Molecules, 24:20-24.

Zhou WW, Li J, Hu J et al (2018). Distribution,Sources,and Ecological Risk Assessment of Polycyclic Aromatic Hydrocarbons (PAHs) in Soils of the Central and Eastern Areas of the Qinghai-Tibetan Plateau. Envirin Sci, 39:1413-1420.

Zhou C, Liu G, Wu D (2014) Mobility behavior and environmental implications of trace elements associated with coal gangue, A case study at the huainan coalfield in china. Chemosphere, 95,193-199．

Figures

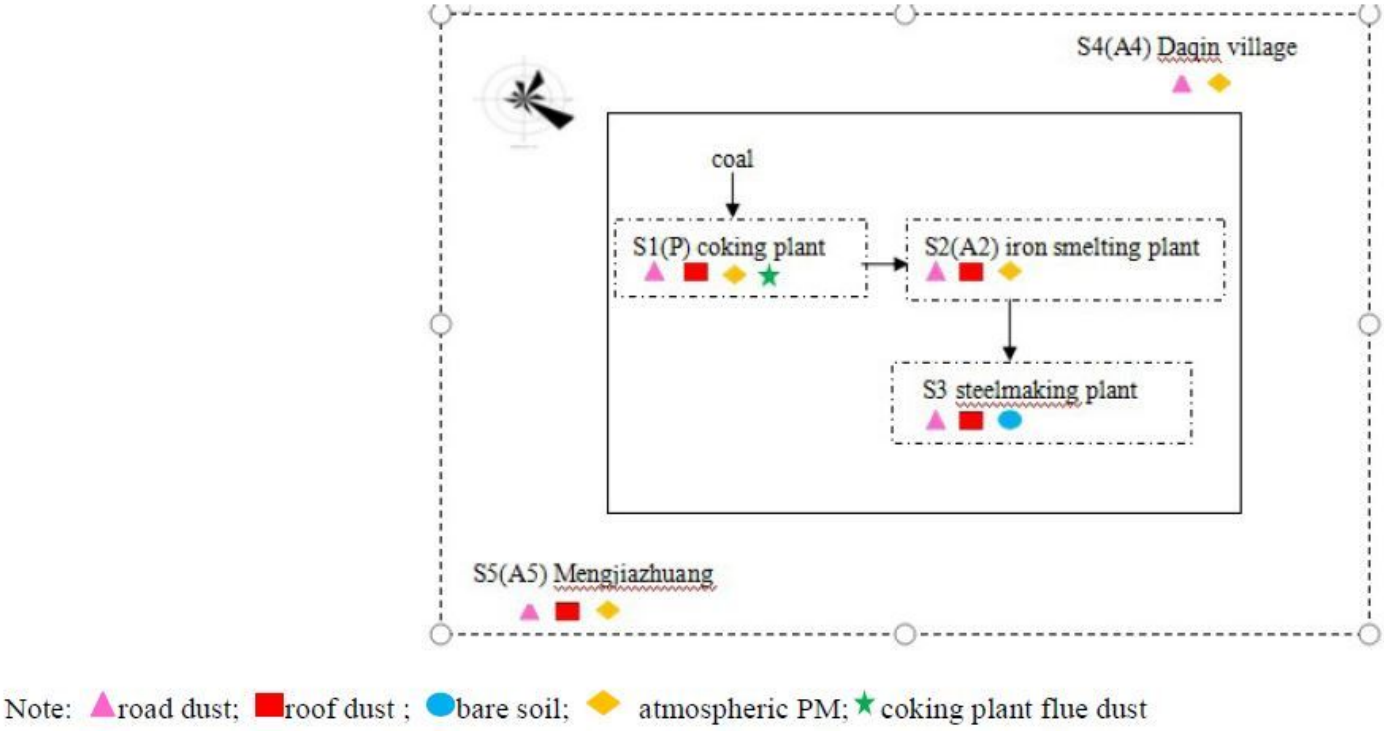

Figure 1

Spatial distribution of the sampling sites

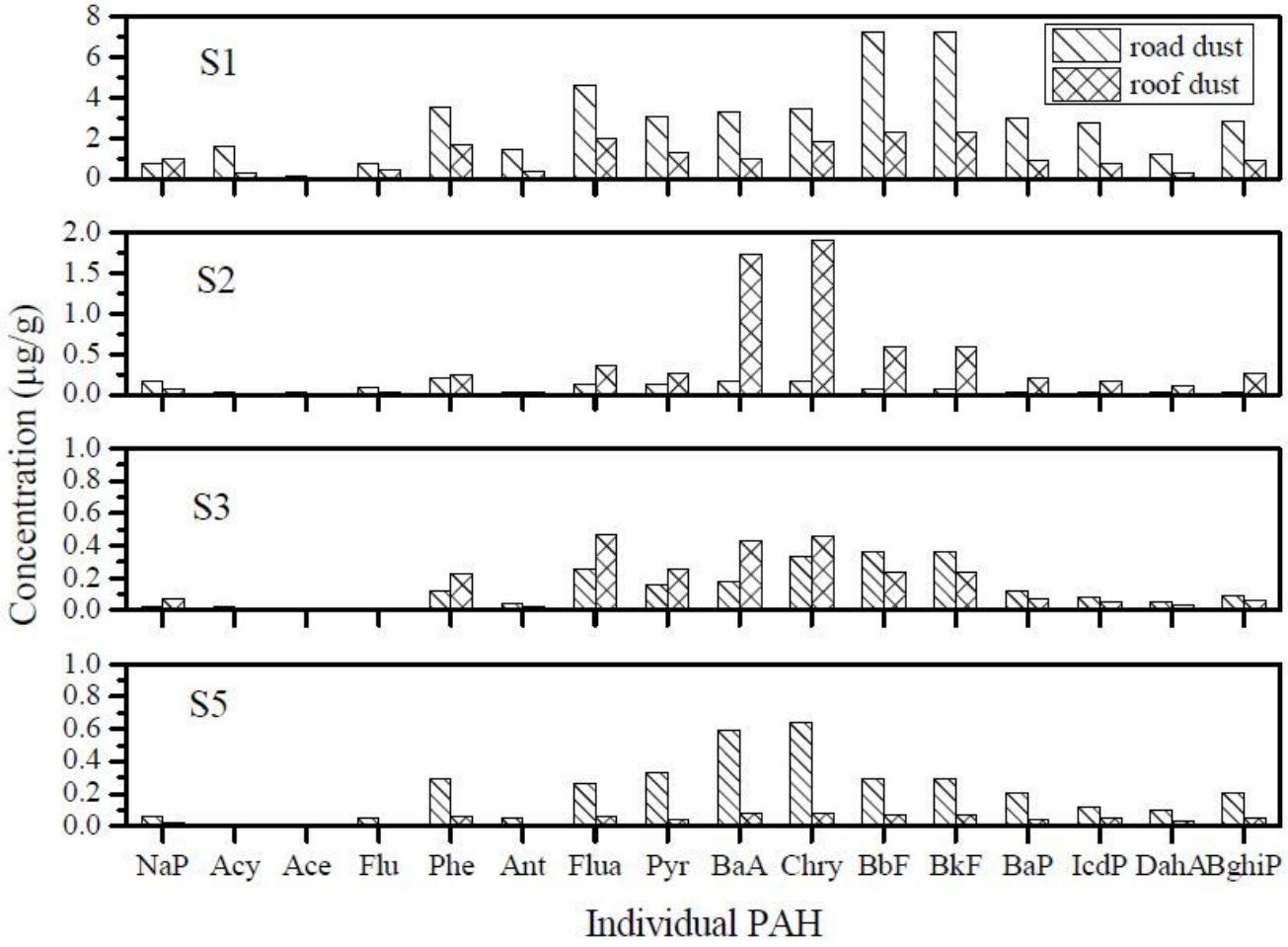

Figure 2

Distribution of PAH of road dust and roof dust at various sampling sites

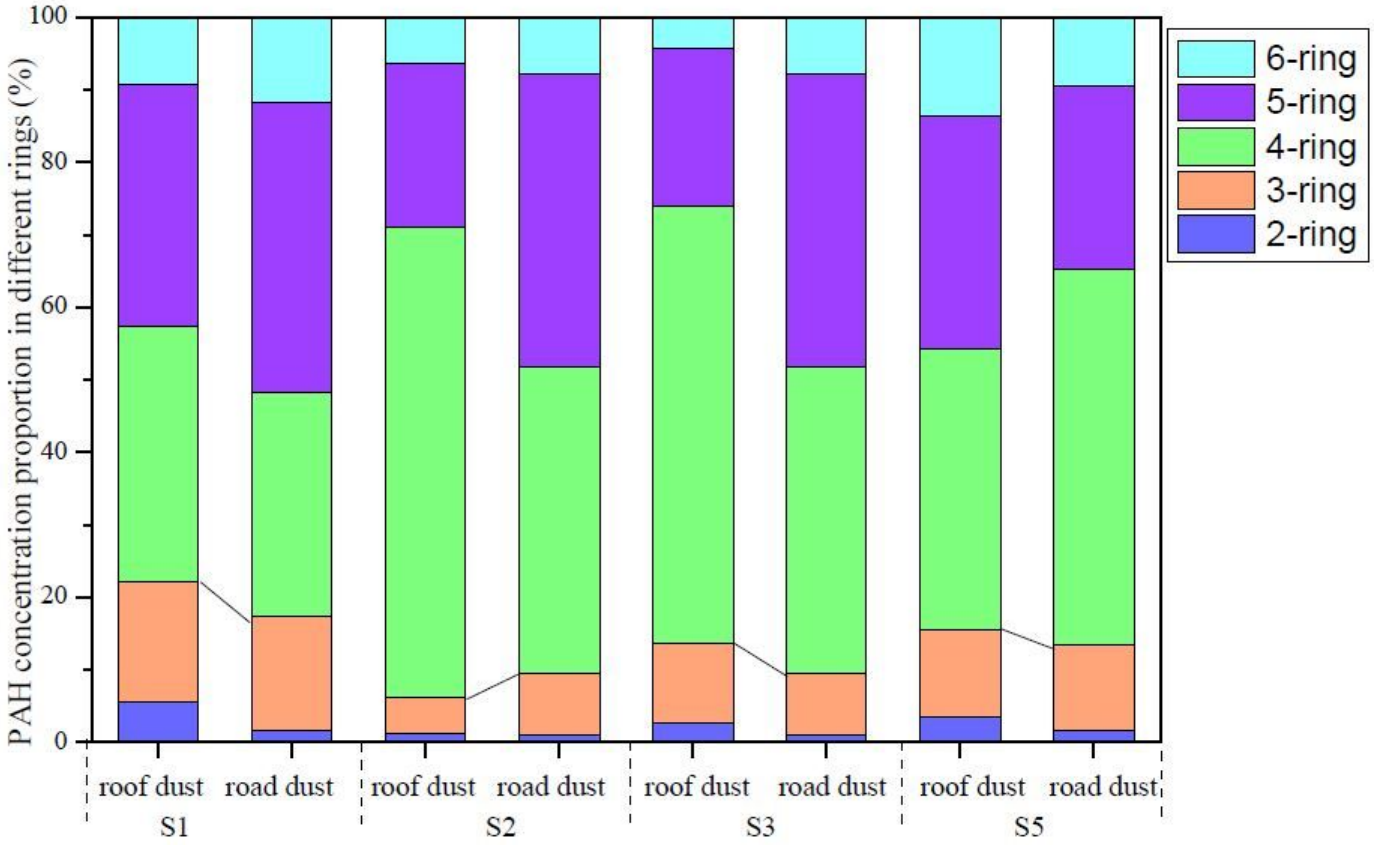

Figure 3

Distribution of PAH with various rings at the sampling sites

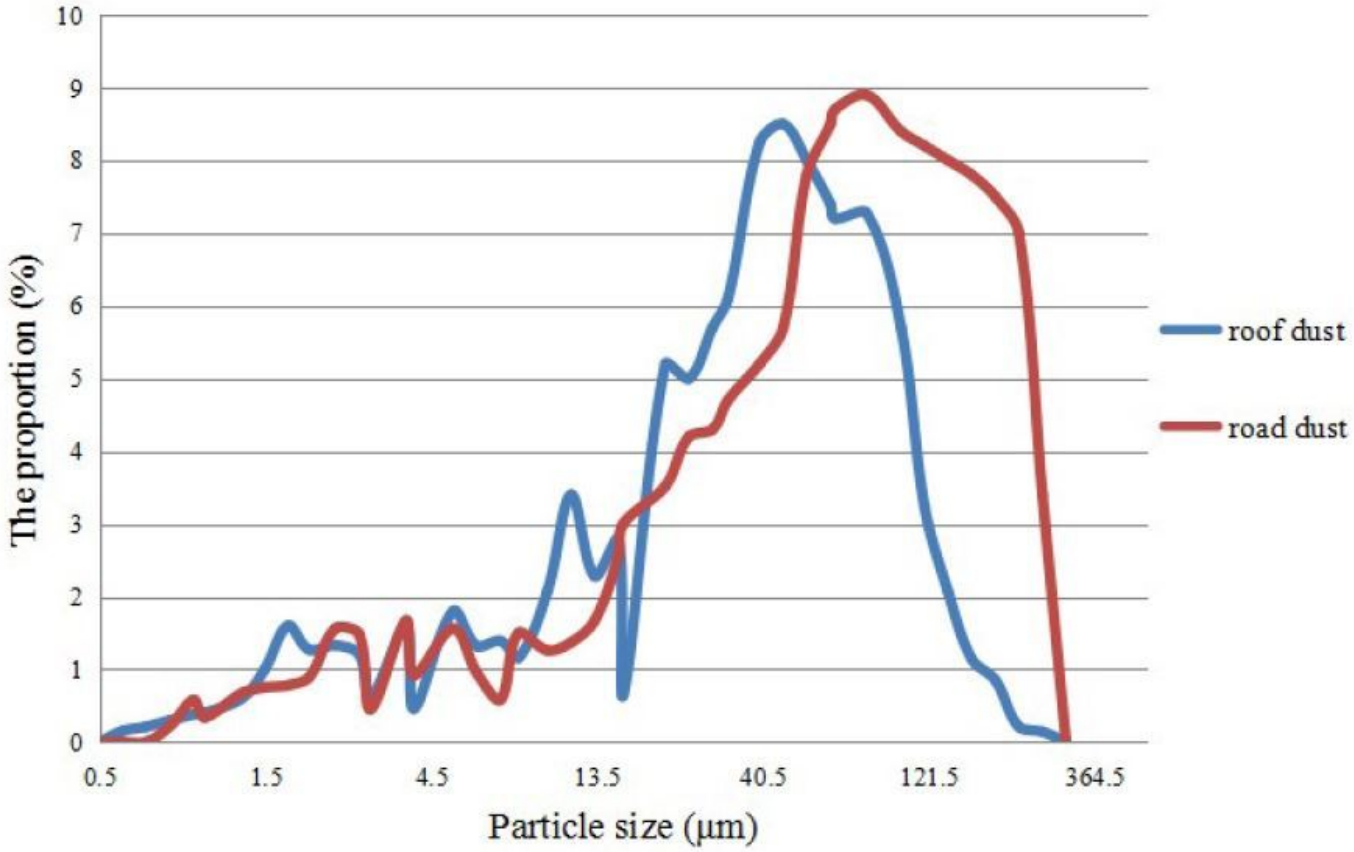

Figure 4

Distribution of particle size in roof dust and road dust

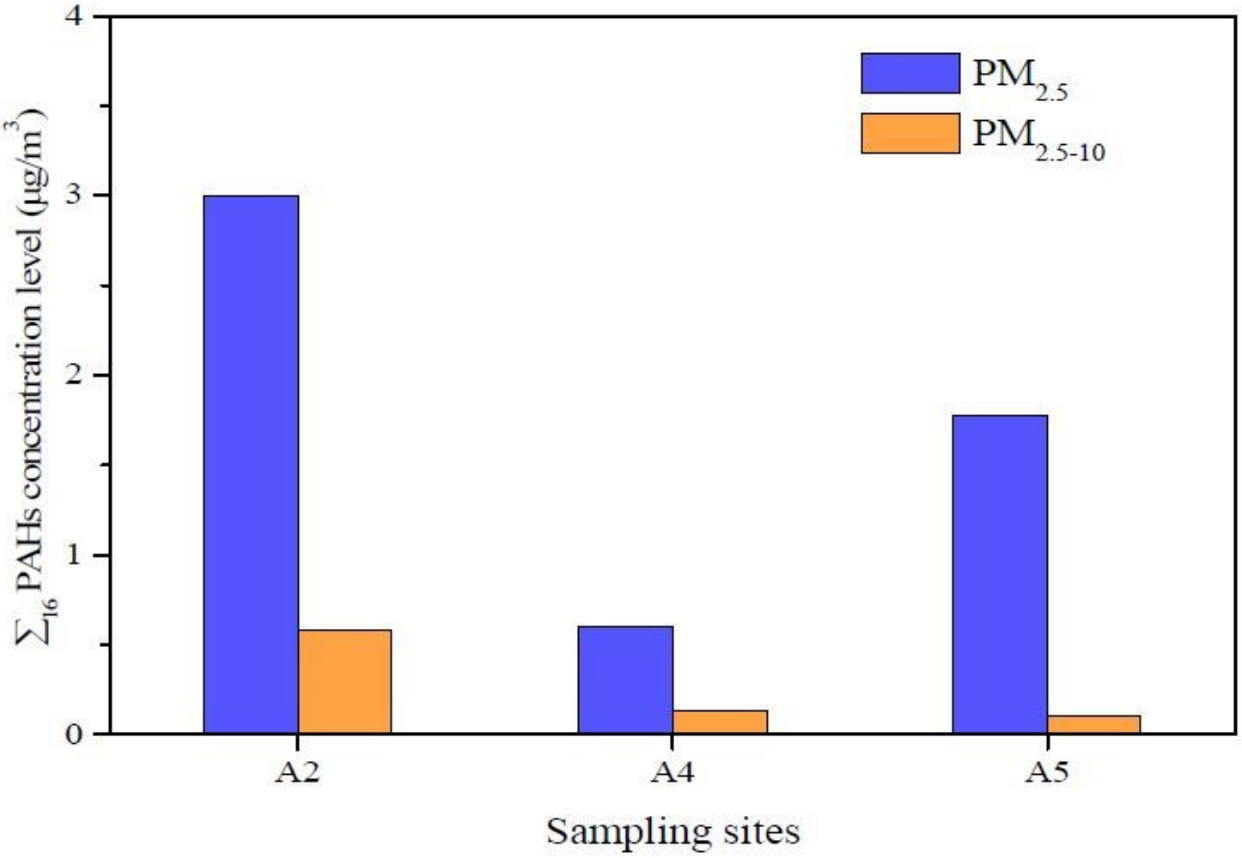

Figure 5

Σ16 PAHs concentrations in atmospheric particulate matter (PM), roof dust, and road dust at different sampling sites

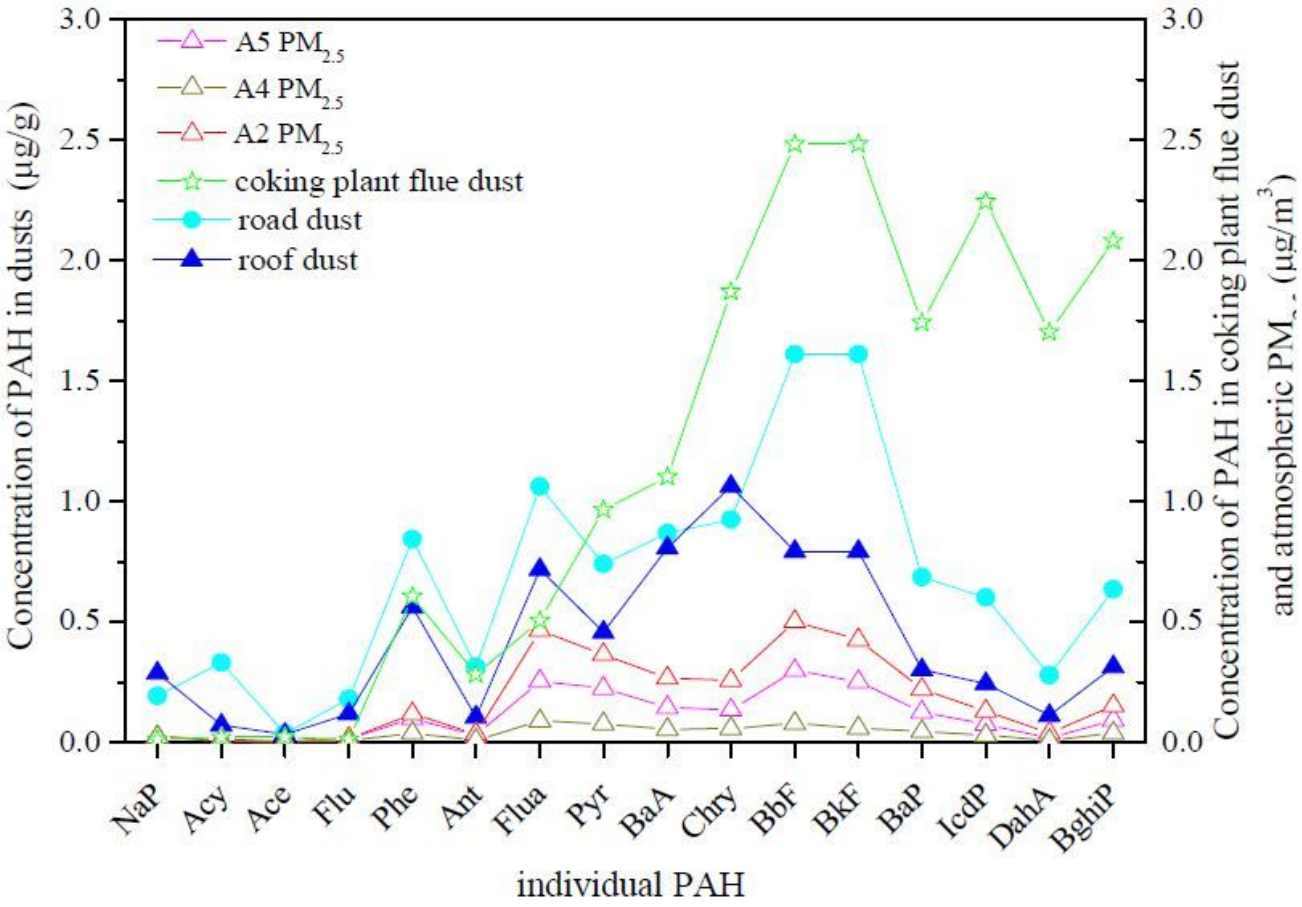

Figure 6

Individual PAH concentrations in dust, coking plant, flue dust, and atmospheric PM2.5